The dependence of the association rate of surface-attached adhesion molecules CD2 and CD48 on separation distance

Anne Pierres[a], Anne Marie Benoliel[a], Pierre Bongrand[a,*], P. Anton van der Merwe[b]

[a]*Laboratoire d'Immunologie, INSERM U 387, Hôpital de Sainte-Marguerite, BP 29, 13274 Marseille Cedex 9, France*
[b]*MRC Cellular Immunology Unit, Sir William Dunn School of Pathology, University of Oxford, Oxford OX1 3RE, UK*

Received 4 December 1996

Abstract The kinetics of bond formation between spherical beads coated with CD48 and CD2-derivatized surfaces was studied with a flow chamber. For a given shear rate, the binding frequency was exquisitively sensitive to the particle velocity. Flow equations were used to derive the particle-to-surface distance from the velocity, thus yielding a relationship between this distance and the binding rate. Numerical values of the binding site densities allowed absolute determination of the rate of association between two invididual molecules as a function of the distance between attachment points. In our model, this rate was about 0.03 s^{-1} at 10 nm separation, and it was inversely proportional to the cube of the distance.

Key words: Adhesion; Binding kinetics; CD2; CD48; Flow chamber

1. Introduction

Many important biological functions, such as cell migration on a surface, particle uptake by phagocytic cells, or antigen recognition by circulating lymphocytes, are dependent on the capacity of the cell to establish rapid adhesion with various surfaces [1–3]. Experiments performed with different model systems have shown that a minimal contact time of several seconds might be required to allow lectin-mediated thymocyte agglutination [4] or phagocyte adhesion to glass surfaces [5]. However, the adhesion of platelets [6] or leukocytes [7] to endothelial cells may occur within a hundredth of a second. High rates of bond formation between red cells and antibodies have also been reported [8].

Thus, there is a need for experimental data on the kinetics of bond formation and dissociation between cell surface adhesion receptors. During the past few years, experimental works based on micromanipulation [9], hydrodynamic flow [10–13] or atomic force microscopy [14,15] have allowed direct visualization of the detachment of surfaces linked by a few (or even one) molecular bond(s) and subjected to a calibrated distractive force, thus yielding an estimate of the lifetime of individual ligand–receptor bonds. However, it is more difficult to measure bond formation due to the requirement for simultaneous control of surface-to-surface approach (in order to know the exact time of contact) and application of a distractive force (in order that bond rupture might result in detectable surface separation). Further, this force must be weak enough not to prevent bond formation. A laminar flow chamber may be a suitable tool for achieving this goal: if individual receptor-bearing particles are driven along receptor-coated surfaces by a hydrodynamic force of a few piconewtons, i.e. much less than the strength of many ligand–receptor bonds [9,12,14,16], individual binding events may be detectable provided time and position are measured with sufficient accuracy. Intermolecular contact frequency may be calculated if the surface density of adhesion molecules and particle-to-surface distance are estimated.

The aim of the present work was to obtain quantitative information on the rate of bond formation between receptor-bearing spheres and ligand-coated surfaces separated by a varying distance in presence of hydrodynamic forces. The floor of a flow chamber was coated with recombinant CD2 molecules (an adhesion receptor found on T lymphocytes [17,18]) and beads were coated with high levels of CD48 (a ligand of CD2) through a flexible molecular link of about 16 nm in length. Beads were subjected to low shear rate (between 11 and 56 s^{-1}) in order that the formation of a single bond might arrest a moving particle [19]. Under conditions of high ligand density, arrest duration was expected to be increased by the formation of multiple bonds. The motion of individual beads was monitored with high spatial ($\approx$0.05 μm) and temporal (0.02 s) resolution. The frequency of bead arrests was determined as a function of bead velocity, which was related to the distance between the sphere and the surface through basic results from fluid mechanics [20]. A quantitative relationship between binding rate and particle-to-surface distance could thus be obtained.

2. Materials and methods

2.1. Molecules and surfaces

Our experimental system was fully described in a previous report [19]. Particles were streptavidin-coated spheres of 2.8 μm diameter (Dynabeads M280, Dynal France, Compiègne). They were first coated with biotinylated [21] mouse anti-rat CD4 (OX68, a previously described IgG2a, [22]). In some cases, this antibody was diluted with an irrelevant biotinylated anti-HLA-DR antibody (Immunotech, Marseille, France, an IgG2b produced by clone B8.12.2). Beads were then incubated in a solution of sCD48-CD4 [23] which comprised two extracellular immunoglobulin domains of rat CD48 (residues 1–195 of the mature protein) linked to two immunoglobulin domains of rat CD4 (residues 183–366). Previous calibration experiments showed that antibody-coated beads displayed about 3460 binding sites/μm^2 [13].

Glass surfaces were thus coated as previously described [24] with polylysine hydrobromide (Sigma, St. Louis, MO; 375 000 molecular weight). They were then washed and incubated with glutaraldehyde (Sigma), then soluble recombinant rat CD2 (residues 1–177 [25]). Finally, unreacted aldehyde groups were blocked with glycine. The surface density of CD2 reactive sites was determined with confocal microscopy [24] by sequential treatment with anti-CD2 monoclonal antibody (OX34 [26]) and fluorescent anti-mouse kappa chain antibodies (rat IgG1κ, clone H139.52.1, supplied by Immunotech, Marseille). Treated surfaces displayed about 800 kappa sites per μm^2.

*Corresponding author. Fax (33) 491-75-73-28

PII S0014-5793(97)00060-4

2.2. Flow chamber

Our apparatus has previously been described [13,27]. The chamber was a rectangular cavity of $6\times17\times0.16$ mm^3. The bottom CD2-coated surface was stuck with silicon glue. The flow was generated by a 1 ml syringe mounted on a syringe holder driven by a synchronous electric motor and endowed with digital velocity settings (Razel, supplied by Bioblock, Illkirch, France). The wall shear rate G was calculated with the following standard formula:

$$G = 6Q/wh^2 \quad (1)$$

where Q is the flow rate, and w and h are the chamber width and height, respectively. Experimental check of the flow properties has previously been described [28].

The chamber was set on the bottom of an inverted microscope equipped with a videocamera and the motion of flowing particles was recorded with a videocassette recorder for delayed analysis.

2.3. Position determination and image analysis

Accurate real-time determination of particle location was performed after processing images with a PCVision+ digitizer (Imaging Technology, Bedford, MA) mounted on a desk computer, using a custom-made assembly language sofware developed in the laboratory as previously described [29]. This allowed calculation of the coordinates of the centroid of moving particles with a resolution of about 0.05 μm [29], and a sampling frequency of 50 Hz, higher than standard video rate. The object area was also calculated and recorded in order to detect potentially artefactual events such as particle collisions.

2.4. Motion analysis

Since more than 2500 individual trajectories and 350 000 positions were recorded, dedicated sofware had to be developed for data processing. It was found convenient to define as arrested particles moving by less than 0.34 μm (i.e. 2 pixel units) during a time interval of 60 ms (or 120 ms when the wall shear rate was lower than 22 s^{-1}). All detected arrests were then examined in order to exclude any possible artifact (see Section 3).

In order to achieve sufficient accuracy, the 'instantaneous velocity' was calculated at any time t as the mean velocity during the period of 160 ms preceding time t. This calculation was performed for all time points that were preceded by a 160 ms period without arrest. Then, velocities were ordered in 50 classes of 1 μm/s width and two histograms were constructed for the velocity distribution of (i) all time points, and (ii) all time points preceding an arrest (Fig. 1). The binding frequency for a given velocity class was thus calculated as the ratio:

$$\text{Binding Frequency} = N_A/(N_T\times\Delta t) \quad (2)$$

where N_T and N_A are the total number of time points and the number of time points with arrests within the given velocity class, and Δt is the duration of a time step, i.e. 0.02 s.

The distance δ between the flowing particle and surface was calculated using a formula obtained by interpolation of numerical results from fluid mechanics [19,30]:

$$\delta/a = \exp(-3.5103\ln^2(U/aG) + 2.4522\ln(U/aG) - 1.6359) \quad (3)$$

where a and U are the particle radius and velocity, and G is the wall shear rate. This formula was found to hold (with a squared error <0.001) when U/aG ranged between 0.4 and 1.

2.5. Error estimation

It was essential to check that the experimental determination of all parameters involved in Eqs. (2) and (3) was accurate enough to warrant numerical treatment. The main sources of errors were as follows.

2.5.1. Binding frequency. The main uncertainty in calculating the binding frequency (Eq. 2) was due to the statistical error involved in counting rare events. Since N_A was much lower than N_T (Fig. 1), the coefficient of variation of the binding frequency was $1/\sqrt{(N_A)}$ [31].

2.5.2. Derivation of distance from velocity measurements. Two main errors must be considered when Eq. 3 is used to derive the particle-to-surface distance from U/aG: there is a random experimental error in determining U/a, and there is a systematic error linked to the assumption that the shear rate G is constant, which is only an approximation in the flow chamber.

2.5.3. Velocity determination. The particle velocity U was calculated by measuring the displacement L during a period of time Δt equal to 0.16 s. The accuracy of distance determinations was studied experimentally. Particles were coated with anti-CD2 antibodies and driven along CD2-derivatized surfaces in the chamber flow: they exhibited numerous arrests longer than several tens of seconds. Eighteen arrested particles were monitored for about 50 s, for determination of position at regular intervals of 0.16 s. The root mean squared variation of the x coordinate (i.e. the coordinate along an axis parallel to the flow) was then determinated. The mean value was 0.044 μm: it was used as an estimate of the displacement error ΔL. The velocity error was then estimated as $\Delta L/\Delta t = 0.275$ μm/s.

2.5.4. Variations of the shear rate G. The shear rate was determined as previously described [10,27] by measuring the velocity of beads flowing at various distances from the chamber floor. In accordance with previous results, G appeared linearly dependent on the distance to the wall when this was less than about 6 μm (not shown). However, since minimal variations of G could cause significant variations of (Eq. 3) a theoretical analysis was required to obtain a quantitative estimate of the expected error.

2.5.5. Distance to the wall. It is easily shown from basic principles of fluid mechanics [32] that the velocity profile in a parallel plate chamber of infinite width and height h is parabolic, i.e.:

$$v = Gz(1-z/h) \quad (4)$$

where z is the distance to the chamber floor, v is the fluid velocity and G is the wall shear rate. Due to the linearity of Navier Stokes equations at low Reynold's number, which is the basis of Goldmann's calculation [20], the neglect of the squared term in the right-hand side of Eq. 4 is equivalent to underestimating the velocity of a particle, with an error ΔU_G equal to the velocity of a sphere located at the same distance from the surface, in a flow with a velocity profile:

$$v(z) = Gz^2/h \quad (5)$$

Although the exact determination of the motion of a sphere in this flow has not been achieved at the present time, it is reasonable to use as an estimate of the error the fluid velocity at the center of gravity of the sphere, yielding:

$$\Delta U_G = G(\delta + a)^2/h \quad (6)$$

2.5.6. Distance to the edge of the chamber. Since the width w of the chamber was finite, the wall shear rate G at any point M was expected to depend on the distance y between M and the chamber axis (the y axis is parallel to the chamber floor and perpendicular to the flow). Assuming parabolic variation of the flow rate with respect to y, an approximate estimate for the variation of parameter G near the chamber axis is:

$$G(y) = G(0)(1-4(y/w)^2) \quad (7)$$

Since the microscope was carefully focussed on the chamber axis, the maximum variation of y was $\omega = 33$ μm, corresponding to half the height of the microscope field. Since the chamber width w is 6000 μm, the maximum error of $G(y)$ is of order of 0.0001, which is negligible as compared to other errors.

We used Eq. 3 to determine numerically the error involved in the determination of parameter δ when velocity errors ΔU and ΔU_G were added. Using a wall shear rate of 22 s^{-1} (corresponding to the estimates presented in the paper), U was systematically varied from 12 to 31 μm/s, corresponding to an increase of the particle-to-substrate distance δ from 1.2 to 277 nm. The relative error in δ was a decreasing function of δ, with numerical values of respectively 49%, 30%, 20% and 14% when δ was 1.2, 7.6, 26.5 and 63.7 nm.

2.6. Use of particle binding rate to calculate association rates between surface-bound molecules

Let $k(z)$ be the association rate between a surface-bound CD2 molecule and an anti-CD4–CD4–CD48 complex whose anchoring points are separated by a distance z. The association rate $L(z)$ between the complex and a planar surface coated with CD2 molecules at surface density σ_s is:

$$L(z) = \int_z^\infty k(\rho)\times\sigma_s\times2\pi\rho d\rho \quad (8)$$

where ρ is the distance between the complex on the bead and any point on the plane. Further, the binding rate $P(\delta)$ between the surface

and a bead of radius a coated with anti-CD4–CD4–CD48 complex as surface density σ_b is:

$$P(\delta) = \int_{\delta}^{\infty} L(z) \times \sigma_b \times 2\pi a dz \quad (9)$$

(the upper bound of the integral was written as infinity since the particle size is much larger than the range of molecular interactions).

Eqs. (8) and (9) allow straightforward derivation of function k by double derivation of P.

3. Results

3.1. Flowing particles display numerous arrests of varying duration due to CD2–CD48 interaction

CD48-bearing beads were driven along CD2-coated surfaces and trajectories were recorded. Typical examples are shown on Fig. 2. Particles displayed periods of fairly regular motion separated by short arrests of widely varying duration, ranging between a few tens of a millisecond (Fig. 2A) and more than 10 s. These arrests were easily discriminated from artifactual events (Fig. 2B) due to the passage of another particle with different flowing velocity or change of particle brightness, since in the latter cases recorded particle area displayed marked alteration (Fig. 2B).

It was important to verify that arrests actually represented CD2–CD48 interactions. As previously described [19], it was checked that (i) beads coated by anti-CD2, not anti-CD4 of similar immunoglobulin class, interacted with the substratum, and (ii) addition of CD4–CD48 chimera to anti-CD4-coated beads dramatically increased the number of arrests. Interestingly, essentially all arrests mediated by anti-CD2 antibodies were durable (>10 s, not shown) whereas CD48–CD2 interactions were much more transient.

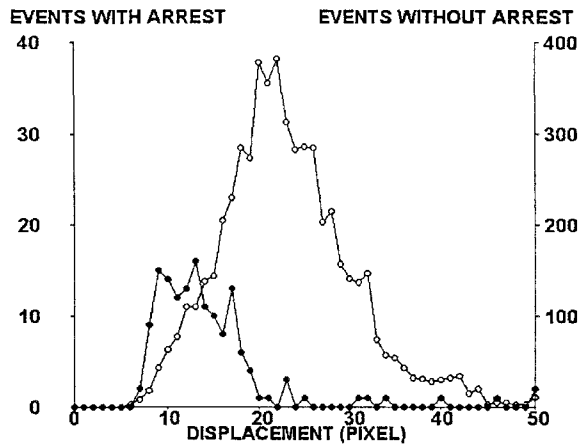

Fig. 1. Velocity distribution of flowing particles. In a representative experiment, CD48-coated spheres were driven along CD2-derivatized surfaces with a wall shear rate of 22 s^{-1}. Seventy-four individual particles were monitored, and their position was recorded every 0.02 s, yielding a total of 18 890 points. A particle was defined as having arrested at any point when it moved by less than 0.34 μm during the following 60 ms. The mean velocity at any point was then calculated as the mean velocity during the preceding 160 ms. This calculation was performed on 5471 points sharing the property that no arrest was detected during the preceding 160 ms. The frequency distribution of these mean velocities is shown for all these 5471 points (○, right-hand scale) or only the 144 points preceding an arrest (●).

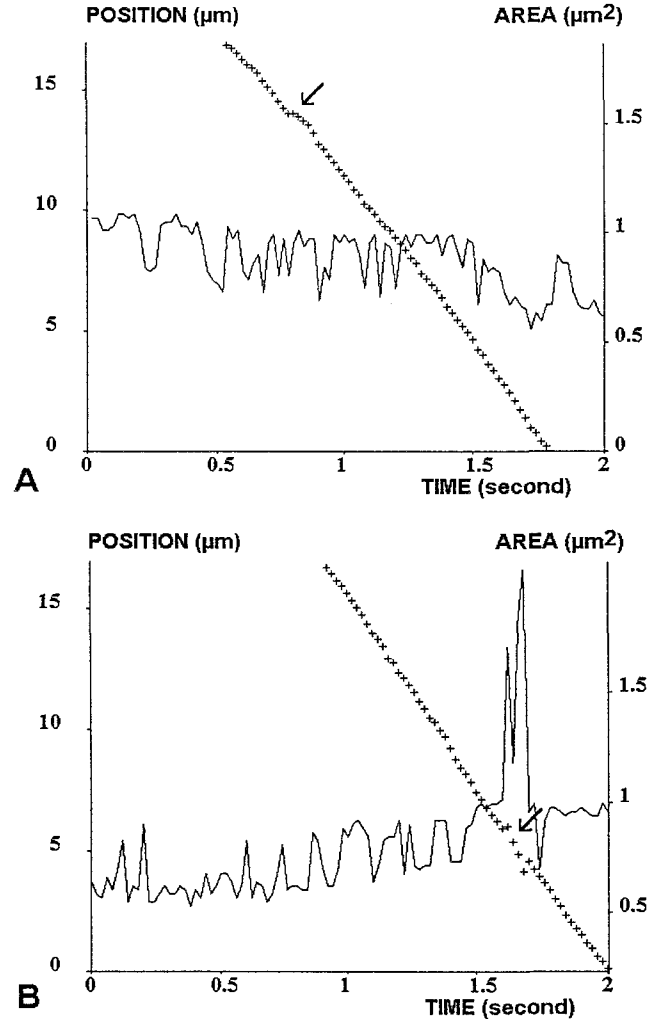

Fig. 2. Typical trajectories. Two CD48-coated spheres were monitored during their passage along CD2-derivatized plates under a wall shear rate of 22 s^{-1}. The position parallel to the flow was determined every 0.02 s (crosses) together with particle surface area (smooth line). A typical short-term arrest of about 60 ms duration is shown on (A, arrow). An artefact is shown on (B, arrow): the particle was caught up with a more rapid sphere yielding four positions indicative of higher velocity (arrow) with concomitant increase of measured area.

3.2. Under a given shear rate, arrest frequency is strongly correlated to particle velocity

Velocity distribution plots (Fig. 1) were used to derive the dependence of adhesion frequency on particle velocity. A typical curve (showing data obtained in a representative experiment out of three done with a wall shear rate of 22 s^{-1}) is shown on Fig. 3A. Adhesion frequency was sharply dependent on cell velocity, since this parameter displayed a 10-fold drop when the velocity increased by a factor of two.

This set of results was used to derive a tentative relationship between adhesion frequency and particle-to-surface distance (Fig. 3B). Experimental points were fitted to a second-order polynomial relationship between binding adhesion frequency and the logarithm of particle to substrate distance (Fig. 3B). This curve was used to derive a relationship between intermolecular association rate k and distance, using Eqs. (8) and (9). As shown on Fig. 3C, k was fairly proportional to the inverse

of the cube of the distance. The binding rate was about 0.03 s^{-1} at 10 nm separation.

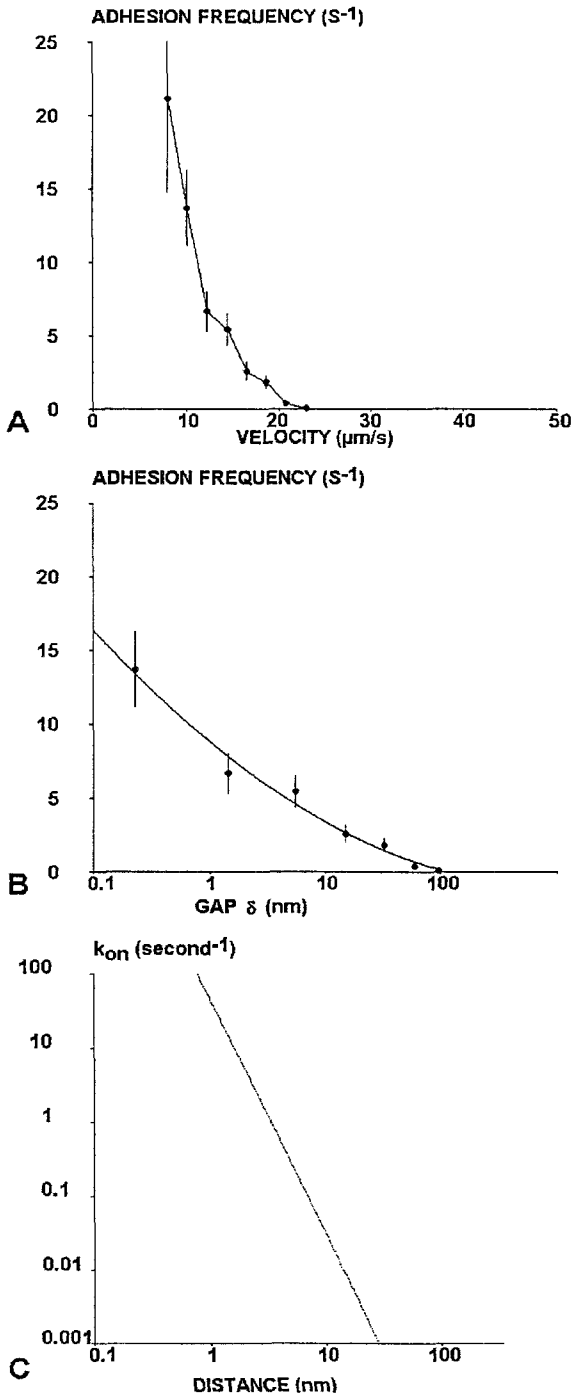

Fig. 3. Relationship between adhesion frequency and particle velocity or particle-to-surface distance. The dependence of bead adhesion frequency on velocity in presence of a wall shear rate of 22 s^{-1} was calculated after ordering velocities in sequential classes of 2 µm/s width (A). Eq. (3) was then used to relate binding frequency and particle-to-surface distance (δ), as shown in (B). Vertical bars represent twice the calculated standard error. The theoretical curve obtaned by fitting experimental values (B, continuous line) was used to derive the dependence of molecular binding rate on separation distance, using Eqs. (8) and (9). The result is shown on (C).

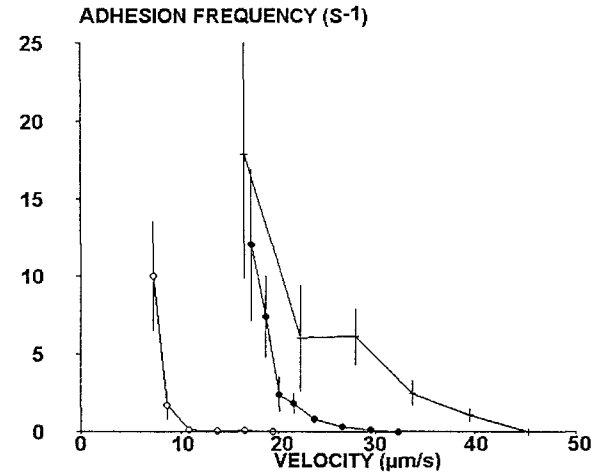

Fig. 4. Dependence of adhesion frequency on particle velocity and wall shear rate. In three separate experiments, CD48-coated particles were driven along CD2-derivatized surfaces with a wall shear rate of 14 s^{-1} (○), 28 s^{-1} (●) and 56 s^{-1} (+). Adhesion frequencies were then calculated as explained in the legend to Fig. 3 and plotted versus velocity.

3.3. Binding probability is more dependent on cell-to-surface distance than wall shear rate

It was important to know whether the results shown on Fig. 3 actually reflected the dependence of arrest frequency on particle-to-surface distance or the binding process was exquisitely sensitive to the absolute particle velocity. This question was addressed by varying the wall shear rate over a 4-fold range and measuring arrest frequency. Representative curves are shown on Fig. 4. Clearly, the binding frequency was more tightly correlated to the ratio between particle velocity and wall shear rate (U/G) than to the absolute velocity.

4. Discussion

The purpose of the present paper was to present an experimental determination of the on-rate of bond formation between receptor-bearing particles and ligand-coated surfaces. The CD2–CD48 interaction was chosen as a suitable model since it mediates cell–cell adhesion and it is probably the best characterized cell adhesion molecule interaction [18]. The interaction between soluble CD2 and CD48 has been studied with the powerful plasmon resonance technology [22]. A final point of considerable practical interest is the short half life of the CD2–CD48 interaction: this provides a unique opportunity to observe numerous cell arrests within a single experiment. Indeed, in another model [13,28], particles coated with high antibody densities stopped very rapidly on antigen-coated surfaces, thus perturbing the motion of following spheres; conversely, when antibodies were diluted, it was possible to observe numerous trajectories but only a few arrests could be detected in a single experiment [19].

The data obtained in the present study yielded a quantitative relationship between the velocity of flowing particles and binding efficiency. It is therefore of importance to assess the meaning of this velocity. According to basic principles from fluid mechanics, there is little doubt that the translational velocity U of flowing spheres is negatively correlated to their distance δ from the substratum. It is likely that flowing par-

ticles observed in our study were incompletely sedimented, due to strong repulsive hydrodynamic interactions with the chamber floor [33]. The problem remains to know to what accuracy the quantitative relationship between U and δ that is relevant to smooth spheres [20] can be applied to our model. Prieve and Alexander [34] used Goldman's data [20] to determine the double layer repulsion between colloidal particles and a flat plate: their results were consistent with standard DLVO theory, accounting for colloidal interactions by combining electrodynamic attraction and electrostatic forces in ionic solutions. According to the supplier of the beads used in the present experiments (Dynal), streptavidin behaved as a monolayer of about 4–6 nm thickness deposited on a polymer layer of about 200 nm thickness. Thus, it may not be unreasonable to assume that Eq. (3) should yield a quantitative estimate of parameter δ when this is higher than about 10 nm, whereas lower values should be only considered as semi-quantitative. It would be of obvious interest to check the validity of hydrodynamic theory with optical methods such as interference reflection microscopy [35] or evanescent wave methodology [36].

A quantitative understanding of the relationship between surface separation distance and the on-rate of bond formation is essential for improving our understanding of the process of association between cell surface adhesion molecules. Several authors have modeled these bonds as springs [37–40], but theoretical considerations suggested that the effective spring constant might vary within a very wide range [37]. This information is required to enable two-dimensional binding constants between membrane-bound adhesion molecules [41] to be calculated from three-dimensional (solution) binding constants obtained with soluble forms of these molecules.

More theoretical work is needed to achieve full interpretation of our results, since a comprehensive model of adhesion should consider thermal fluctuations of particle-to-surface distance. Indeed, preliminary experiments have shown that these fluctuations could be demonstrated in our chamber and they were fairly well accounted for by standard diffusion theory [28].

The results described in the present study demonstrate that the flow chamber might in principle yield highly accurate information on the rate of bond formation between surfaces coated with adhesion molecules. The methodology that we have presented allows fairly rapid gathering of data on hundreds of thousands of discrete positions, with a time resolution of 0.02 s and spatial accuracy of order of 0.05 μm. The basic limitation stems from the roughness of interacting surfaces which leads to some uncertainty in distance determination. Further progress will require improved methods for preparing molecularly smooth layers [42] as well as incorporation of refined optical techniques for measuring separation distance [35,36].

In conclusion, this report presents, to our knowledge, the first experimental determination of the relationship between the association rate of adhesion molecule and surface separation distance. Application of this powerful methodology to several different molecular systems should substantially improve our understanding of the mechanisms of cell adhesion and structure/function relationships of cell surface receptors.

Acknowledgements: This work was supported by grants from the A.R.C. and the Medical Research Council.

References

[1] André, P., Capo, C. and Bongrand, P. (1990) Bull. Inst. Pasteur 88, 335–361.
[2] Williams, A.F. (1991) Nature 352, 473–474.
[3] Van der Merwe, P.A. and Barclay, A.N. (1994) Trends Biochem. Sci. 19, 354–358.
[4] Capo, C., Garrouste, F., Benoliel A.M., Bongrand, P., Ryter, A. and Bell, G.I. (1982) J. Cell Sci. 56, 21–48.
[5] Mège, J.L., Capo, C., Benoliel, A.M. and Bongrand, P. (1986) Cell Biophys. 8, 141–160.
[6] Baumgartner, H.R. (1973) Microvasc. Res. 5, 167–180.
[7] Lawrence, M.B., McIntire, L.V. and Eskin, S.G. (1987) Blood 70, 1284–1290.
[8] Xia, Z., Goldsmith, H.L. and van de Ven, T.G.M. (1993) Biophys. J. 65, 1073–1083.
[9] Evans, E.A., Berk, D. and Leung, A. (1991) Biophys. J. 59, 838–848.
[10] Kaplanski, G., Farnarier, C., Tissot, O., Pierres, A., Benoliel, A.M., Alessi, M.C., Kaplanski, S. and Bongrand, P. (1993) Biophys. J. 64, 1922–1933.
[11] Tees, D.F., Coenen, O. and Goldsmith, H.L. (1993) Biophys. J. 65, 1318–1334.
[12] Alon, R., Hammer, D.A. and Springer, T.A. (1995) Nature 374, 539–542.
[13] Pierres, A., Benoliel, A.M. and Bongrand, P. (1995) J. Biol. Chem. 270, 26586–26592.
[14] Florin, E.L., Moy, V.T. and H.E. Gaub (1994) Science 264, 415–417.
[15] Hinterdorfer, P., Baumgartner, W., Gruber, H.J., Schilcher, K. and Schindler, H. (1996) Proc. Natl. Acad. Sci. USA 93, 3477–3481.
[16] Tha, S.P., Shuster, J. and Goldsmith, H.L. (1986) Biophys. J. 50, 1117–1126.
[17] Springer, T.A.M., Dustin, M.L., Kishimoto, T.K. and Marlin, S.D. (1987) Ann. Rev. Immunol. 5, 223–252.
[18] Davis, S.J. and Van der Merwe, P.A. (1996) Immunol. Today 17, 177–187.
[19] Pierres, A., Benoliel, A.M., Bongrand, P. and van der Merwe, P.A. (1996) Proc. Nat. Acad. Sci. USA 93, 15114–15118.
[20] Goldman, A.J., Cox, R.G. and Brenner, H. (1967) Chem. Eng. Sci. 22, 653–660.
[21] Brown, M.H., Preston, S. and Barclay, A.N. (1995) Eur. J. Immunol. 25, 3222–3228.
[22] Van der Merwe, P.A., Brown, M.H., Davis, S.J. and Barclay, A.N. (1993) EMBO J. 12, 4945–4954.
[23] Brown, M.H. and Barclay, A.N. (1994) Protein Eng. 7, 515–521.
[24] Pierres, A., Tissot, O., Malissen, B. and Bongrand, P. (1994) J. Cell Biol. 125, 945–953.
[25] Gray, F., Cyster, J.G., Willis, A.C., Barclay, A.N. and Williams, A.F. (1993) Protein Eng. 6, 965–970.
[26] Williams, A.F., Barclay, A.N., Clarle, S.J., Paterson, D.J. and Willis, A C. (1987) J. Exp. Med. 165, 368–380.
[27] Tissot, O., Foa, C., Capo, C., Brailly, H., Delaage, M. and Bongrand, P. (1992) Biophys. J. 61, 204–215.
[28] Pierres, A., Benoliel, A.M. and Bongrand, P. (1996) J. Phys. III France 6, 807–824.
[29] Pierres, A., Benoliel, A.M. and Bongrand, P. (1995) C. R. Acad. Sci. Paris Life Science 318, 1191–1196.
[30] Pierres, A., Benoliel, A.M. and Bongrand, P. (1996) J. Immunol. Methods 196, 105–120.
[31] Snedecor, G.W. and Cochran, W.G. (1980) Statistical Methods. Iowa State University Press, Ames, IA.
[32] Sommerfeld, A. (1964) Lectures in Theoretical Physics. Vol. II. Mechanics of Deformable Bodies. Academic Press. London.
[33] Dimitrov, D.S. (1983) Prog. Surface Sci. 14, 295–424.
[34] Prieve, D.C. and Alexander, B.M. (1986) Science 231, 1269–1270.
[35] Evans, E., Ritchie, K. and Merkel, R. (1995) Biophys. J. 68, 2580–2587.
[36] Liebert, R.B. and Prieve, D.C. (1995) Biophys. J. 69, 66–73.
[37] Bell, G.I., Dembo, M. and Bongrand, P. (1984) Biophys. J. 45, 1051–1064.

[38] Dembo, M., Torney, D.C., Saxman, K. and Hammer, D. (1988) Proc. Roy. Soc. Lond. B 234, 55–83.
[39] Tözeren, A. and Ley, K. (1992) Biophys. J. 63, 700–709.
[40] Hammer, D.A. and Apte, S.M. (1992) Biophys. J. 63, 35–57.
[41] Dustin, M.L., Ferguson, L.M., Chan, P.-Y., Springer, T.A. and Goland, D.E. (1996) J. Cell Biol. 132, 465–474.
[42] Sackmann, E. (1996) Science 271, 43–48.